Journal of Optoelectronics Engineering, 2015, Vol. 3, No. 1, 1-6
Available online at http://pubs.sciepub.com/joe/3/1/1

DOI:10.12691/joe-3-1-1

Analysis of Strained $Al_{0.15}In_{0.22}Ga_{0.63}As/GaAs$ Graded Index–Separate Confinement Lasing Nano-heterostructure

Swati Jha[1], Meha Sharma[1], H. K. Nirmal[2], Pyare Lal[2], F. Rahman[3], P. A. Alvi[2,*]

[1]Department of Electronics, Banasthali Vidyapith, Rajasthan, India
[2]Department of Physics, Banasthali Vidyapith, Rajasthan, India
[3]Department of Physics, Aligarh Muslim University, Aligarh, U.P., India
*Corresponding author: drpaalvi@gmail.com

Received December 18, 2014; Revised January 17, 2015; Accepted January 22, 2015

Abstract The paper deals with a theoretical insight into the various characteristics of a 0.89 μm $Al_{0.15}In_{0.22}Ga_{0.63}As/GaAs$ strained single quantum well based Graded Index (GRIN) - separate confinement lasing nano-heterostructure. Major emphasis has been laid on the optical and modal gain. Both these gain have been simulated with respect to lasing wavelength, photon energy and current density. In this paper, we have also drawn a comparative picture of the two polarization modes i.e Transverse Electric (TE) and Transverse Magnetic (TM). The maximum optical gain has been observed to be 5557.18 cm^{-1} at the lasing wavelength ~ 0.90 μm and photonic energy ~ 1.36 eV in TE mode and it is only 2760.70 cm^{-1} at the lasing wavelength ~ 0.78 μm and at photonic energy ~ 1.58 eV in TM mode. However, the maximum modal gain has been observed to be 54.65 cm^{-1} in TE mode and it is 27.16 cm^{-1} in TM mode at the same lasing wavelengths and photonic energies respectively at 298 K. The behavior of quasi Fermi levels for the conduction band and valence band has also been studied. Other important parameters like gain compression, differential gain and refractive index profile have also been simulated with respect to carrier density. Anti-guiding factor has been plotted against current density to observe its behavior in order to support the explanation of optical gain simulated.

Keywords: *optical gain, anti-guiding factor, modal gain, current density*

Cite This Article: Swati Jha, Meha Sharma, H. K. Nirmal, Pyare Lal, F. Rahman, and P. A. Alvi, "Analysis of Strained $Al_{0.15}In_{0.22}Ga_{0.63}As/GaAs$ Graded Index–Separate Confinement Lasing Nano-heterostructure." *Journal of Optoelectronics Engineering*, vol. 3, no. 1 (2015): 1-6. doi: 10.12691/joe-3-1-1.

1. Introduction

Separate-confinement heterostructures (SCH) have been used in quantum well based nano heterostructures for quite some time now [1]. Although, the GRIN-SCH architecture has advanced with the use of quaternary alloys like $Zn_xMg_{1-x}SSe$ which imposes photon confinement but some difficulties which concern its synthesis and *p*-type doping are still encountered [2]. GRIN-SCH lasers based on III-V compounds, operating in the red-infrared region of the EM spectrum have already been realized [3]. Laser structures, with either parabolic or linearly graded compositional profile alloys for the confinement of carriers and the optical mode using III-V semiconductors has already been successfully implemented. These designs have enabled the lasers to operate at lower current threshold [4,5,6,7]. However, owing to their cubic symmetry, polarization-enhanced doping is not present in the compositionally graded wave guiding layers of the GRIN-SCHs based on III-V semiconducting material. Yong et al. have studied the material gain in 1.3 μm quantum well InGaAsP, AlGaInAs and InGaAsN lasers [8]. Optical gain and valence effective masses in InGaAlAs and InGaAsP quantum well lasers under compressive strain have been calculated along with refractive index change [9]. Carsten et al. presented that the band gap of QWs can be engineered by varying the composition and changing the well thickness [10]. Lal et al. have simulated lasing characteristics along with material gain for AlGaAs/GaAs nano-heterostructure with in TE and TM mode [11].

2. Theoretical Aspects

Referring the refs. [11,12], the optical gain is found to be inversely proportional to the quantum well width and depends on quasi Fermi function in the conduction and valence band, effective refractive index of the structure, spatial overlap factor, effective mass and Lorentzian lineshape function. Next, optical confinement factor (Γ), which is an important attribute of lasing heterostructures, is defined as the fraction of photons in the waveguide which interact with the active layer material. Mathematically, it is elaborated in [13] as the fraction of optical power of mode contained in the active quantum well layer as;

$$\Gamma = \frac{\int_{-w/2}^{+w/2} |\varepsilon(z)|^2 dz}{\int_{-\infty}^{+\infty} |\varepsilon(z)|^2 dz} \quad (1)$$

where w is the width of the quantum well (active region), $\varepsilon(z)$ is the intensity of electric field in z direction. We always try to optimize this factor for a better lasing structure in order to calculate the mode gain. Researchers have already proposed two methods to increase this quantity. The first is by finely increasing the well width below its critical value. This preserves the advantages of a quasi-2D system while demonstrating a three-dimensional (3D) behavior. The second one and the commonly used strategy is to use SCH. In SCH structures, the optical confinement of the photons is obtained by depositing layers of high-index materials at an optimized distance of the quantum well. Since this architectural implementation involves alloy compounds, carriers get trapped, because of local potential fluctuations which impact their efficiency of injection. So, an alternative and better design was proposed which was better suited for both the photon confinement and the carrier injection. It was termed the graded-index separate-confinement heterostructure (GRIN-SCH). In this architecture, the cladding layers have simultaneously graded refractive index and band gaps. As the carriers flow down along the graded index slopes surrounding the quantum-well layer, as shown in Figure 1, it enables easy collection of carriers in the quantum well.

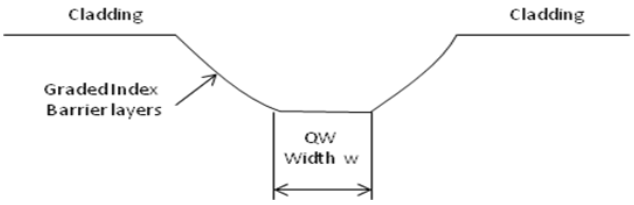

Figure 1. Graded Index profile of a lasing nano-heterostructure.

Modal Gain, denoted as G_M (J), is yet another fundamental characteristic of lasing action in heterostructures and is obtained by multiplying optical gain with the confinement factor and it is given as ;

$$G_M(J) = \Gamma G(J) \quad (2)$$

where G (J) is the optical gain and Γ is the optical confinement factor given in (1). For a single quantum well (SQW), the modal gain is a function of current density [9] and is expressed as;

$$G_M(J) = \Gamma G_0(J)\left[\ln\left(\frac{J}{J_0}\right)+1\right] \quad (3)$$

where $G_0(J)$ is the optimum gain. The modal gain for multiple quantum wells MQW is equal to 'n' times the modal gain for a SQW where 'n' is the number of quantum wells as given as;

$$n\Gamma G(J) = n\Gamma G_0(J)\left[\ln\left(\frac{nJ}{nJ_0}\right)+1\right] \quad (4)$$

In terms of transparency current density, the modal gain for multiple quantum wells can be modified as;

$$n\Gamma G(J) = n\Gamma G_0(J)\left[\ln\left(\frac{nJ}{nJ_0}\right)\right] \quad (5)$$

Lasing action takes place only when the modal gain overcomes the total loss. The required threshold modal gain condition for lasing is expressed as;

$$R_1 R_2 \exp\left[2L\left(n\Gamma G(J)\right) - \alpha_i\right] = 1 \quad (6)$$

The threshold modal gain, $G_{th}(J)$,can be expressed as;

$$G_{th}(J) = n\Gamma G(J) = \alpha_i + \frac{1}{2L}\left[\ln\left(\frac{1}{R_1 R_2}\right)\right] = \alpha_i + \alpha_m \quad (7)$$

where L is the length of the cavity, α_i is the internal optical loss, α_m is the mirror loss which accounts for the transmission losses at both facets, R_1 and R_2 are the reflection coefficients of the two side mirror. The internal loss is a material parameter based on the semiconductor used. The threshold current density is defined as the minimum current required for lasing operation and is defined as;

$$J_{th} = J_{tr} + \frac{G_{th}(J)}{G'(J)} \quad (8)$$

where $G'(J)$ is the differential gain which is defined as material gain per unit current density. Next, the important quantity which describes the behavior of optical gain in the structure is the anti-guiding factor α and is defined as;

$$\alpha = \frac{4\pi\left(-dn/dN\right)}{\lambda(dG/dN)} \quad (9)$$

where (-dn/dN) and (dG/dN) are the differential refractive index and the differential gain of the heterostructure respectively.

3. Device Structure

The model is proposed to have a single quantum well of width 60 Å of quaternary compound $Al_{0.15}In_{0.22}Ga_{0.63}As$ sandwiched between the 50 Å thick graded barrier layers of $Al_{0.2}Ga_{0.8}As$ followed by a cladding of GaAs of 100 Å on a GaAs substrate. The very reason for selecting $Al_{0.15}In_{0.22}Ga_{0.63}As$ layer as a QW in this model is its better material gain, higher refractive index, and higher conduction band discontinuity. Addition of Al increases the band gap energy resulting in the reduced emission wavelength. The resulting quaternary strained QW lasers can operate over a very wide range of wavelengths depending on In and Al compositions [14]. Because of its wide band gap, pure GaAs is highly resistive and when combined with the high dielectric constant it makes GaAs a very good electrical substrate which provides natural isolation between devices and circuits. It has been used to produce (near-infrared) laser diodes since 1962 [15]. Because of almost same lattice constant of GaAs and AlAs the layers have very little induced strain, which allows them to be grown almost arbitrarily thick. It has already been reported that if the active region is grown under Ga-rich conditions assist the development of deep band structure potential fluctuations which ultimately boosts up carrier injection [16,17,18,19,20]. Since the

band-structure potential fluctuations result in localization of the injected excitons even at room temperature, their diffusion and non-radiative recombination is prevented at extended and point defects. As discussed in Refs. [16,17,18,19,20] quantum wells and LEDs with internal quantum efficiency as high as 70 % have already been reported [20].

4. Results and Discussion

To find the envelope functions and corresponding energy states in conduction band of the quantum well, a single effective mass equation has been solved, while for valence band functions the Kohn–Luttinger Hamiltonian equations have been solved. For detailed theory, the references [12,21,22,23] can be referred. For the GRIN-SCH heterostructure, we plot the amplitude of the envelop functions for conduction band (Figure 2), valence band heavy hole (Figure 3) and light hole (Figure 4). From Figure 2, it can be been observed that there is a strong confinement of electrons associated with first energy (CB1) state as compare to the other energy states. Form Figure 3 and 4, it can be seen that the heavy holes associated with second energy state (HH2) are strongly confined as compared to the heavy hole associated with first state, while the light hole belonging to first energy state is strongly confined in the center position of the well as compared with the light hole associated with the second one.

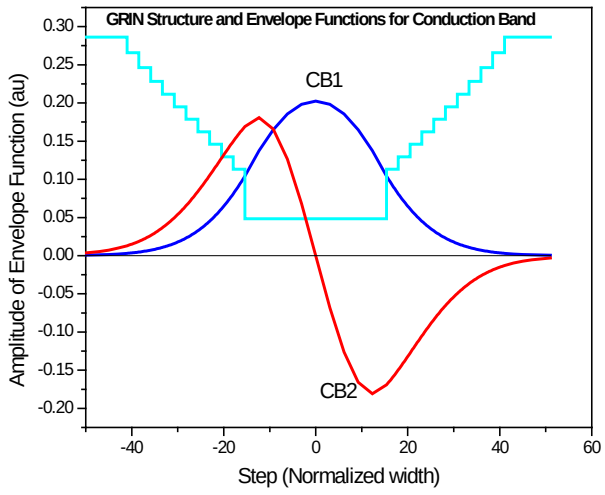

Figure 2. Envelope functions for conduction band.

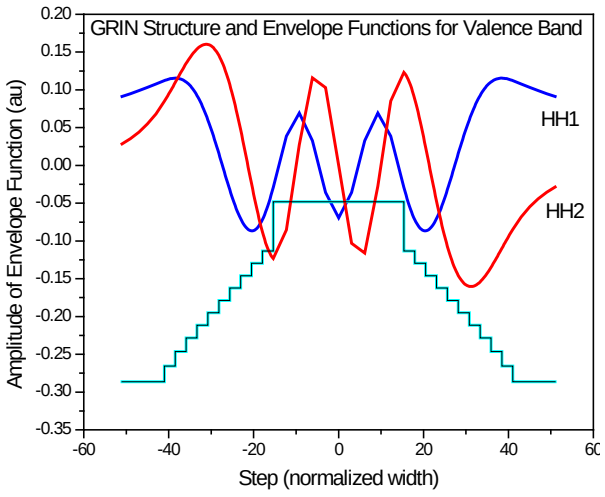

Figure 3. Envelope functions for sub-valence band (heavy holes)

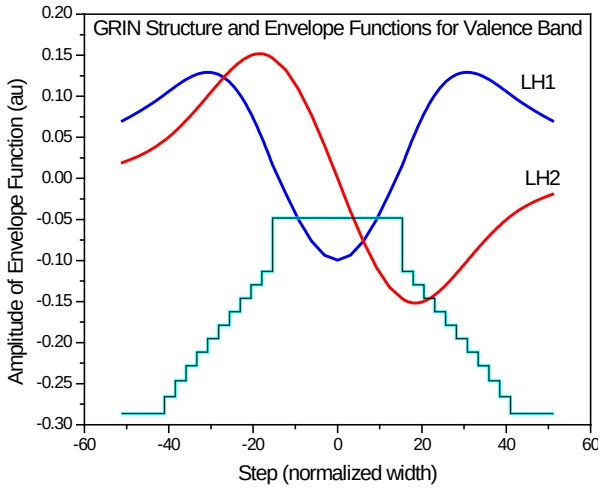

Figure 4. Envelope functions for sub-valence band (light holes)

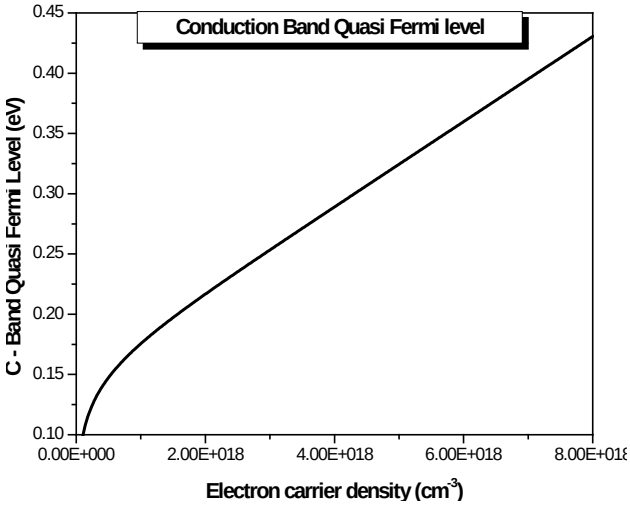

Figure 5. Quasi-Fermi levels as a function of carrier density in the conduction band

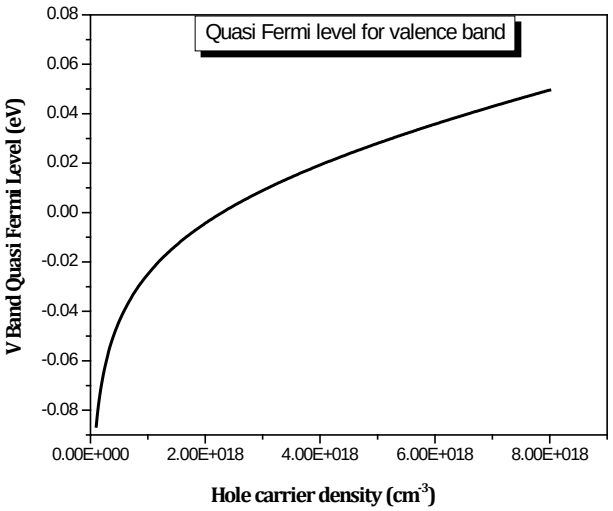

Figure 6. Quasi-Fermi levels as a function of carrier density in the valence band

Quasi-Fermi level, in a semiconductor, describe the population density of electrons and holes separately when their population density is displaced from the condition of equilibrium. In the study of material gain, the knowledge of behavior of quasi-Fermi level plays an important role. These quasi-Fermi-levels of electrons and holes in the respective bands in a quantum well are calculated during

photoluminescence under non-equilibrium condition [24]. The behavior of quasi-Fermi levels as a function of carrier density in the conduction and valence bands have been shown in Figure 5 and Figure 6 respectively for the active layer of $Al_{0.15}In_{0.22}Ga_{0.63}As$ as a quantum well in the nano-heterostructure.

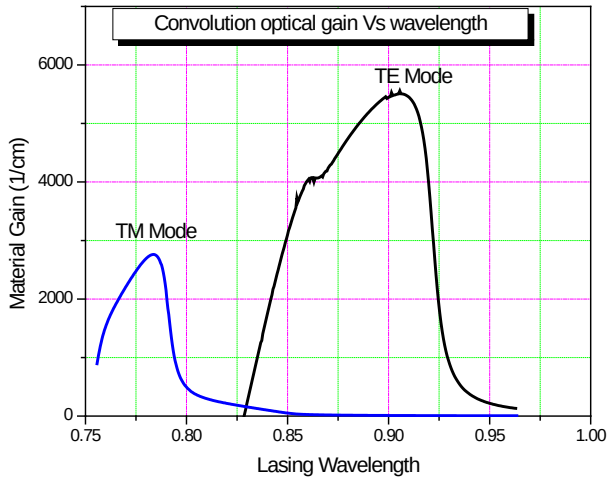

Figure 7. Optical Gain as a function of Lasing wavelength in TE and TM mode

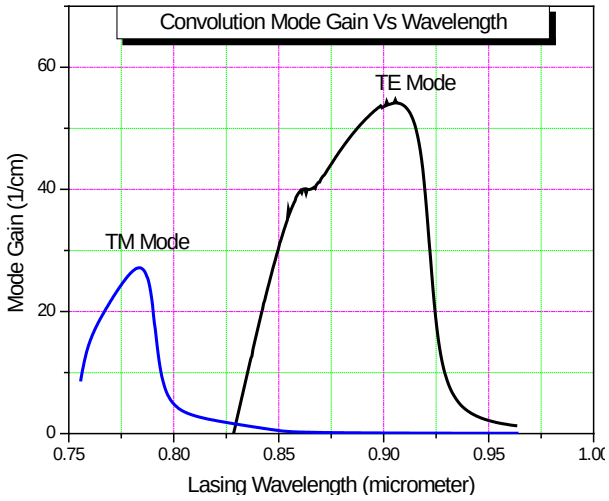

Figure 8. Mode Gain as a function of lasing wavelength in TE and TM mode

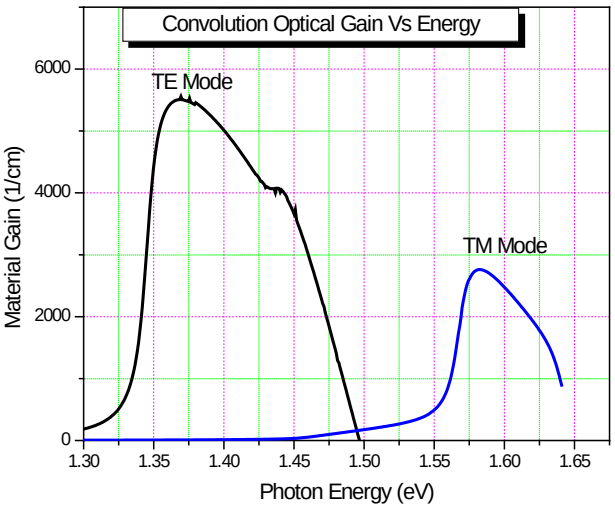

Figure 9. Behaviour of optical gain as a function of photon energy

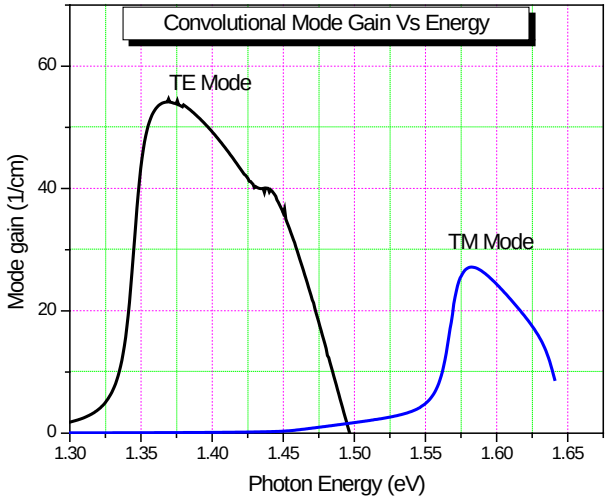

Figure 10. Behaviour of mode gain as a function of photon energy

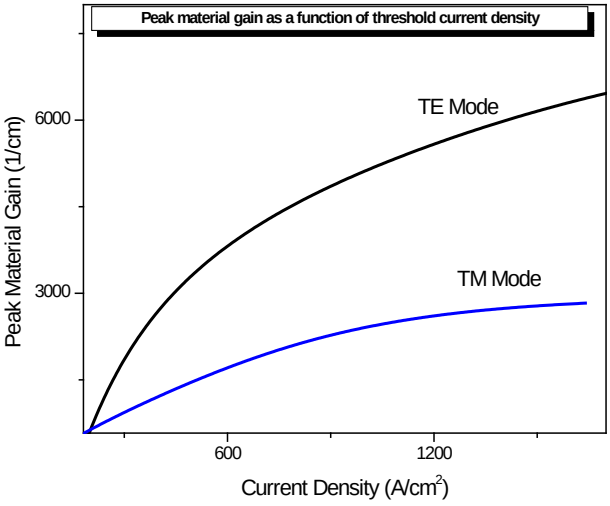

Figure 11. Optical gain as a function of current density

Figure 7 and Figure 8 shows the plot of optical gain versus lasing wavelength and modal gain versus lasing wavelength in both the polarization modes respectively. Here it is noteworthy that TE mode has better gain characteristics than TM mode. The maximum optical gain has been observed to be 5557.18 cm^{-1} at the lasing wavelength ~ 0.90 μm and photonic energy ~ 1.36 eV in TE mode and it is only ~ 2760.70 cm^{-1} at the lasing wavelength ~ 0.78 μm and at photonic energy ~ 1.58 eV in TM mode. The maximum modal gain has been observed to be 54.65 cm^{-1} in TE mode and it is 27.16 cm^{-1} in TM mode at the same lasing wavelengths and photonic energies respectively. Also, there are two peaks in TE mode which may be attributed to transitions involving between electrons occupying first energy state and first heavy holes and light holes. Heavy holes do not create much impact in TM mode and hence we have a single peak. Figure 9 and Figure 10 shows the plot of optical gain versus photon energy and modal gain versus photon energy in both TE and TM modes. If we plot the material or optical gain versus current density, we observe a parabolic increase, as in Figure 11, for initial values of the current density but it saturates afterwards indicating very small or negligible increase in gain with change in current density.

We observe the same trend when modal gain is plotted with respect to current density as shown in Figure 12.

When the behavior of anti-guiding factor is observed with current density (Figure 13), we note a steady growth as expected from eq. (9). Carriers have a unique role to play as far as refractive index is concerned. Hence Figure 14 plots the change in refractive index profile for the two modes when it is plotted against number of carriers.

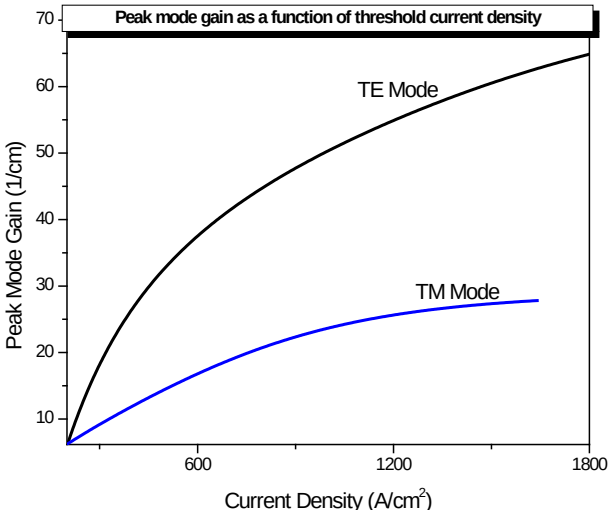

Figure 12. Modal gain as a function of current density

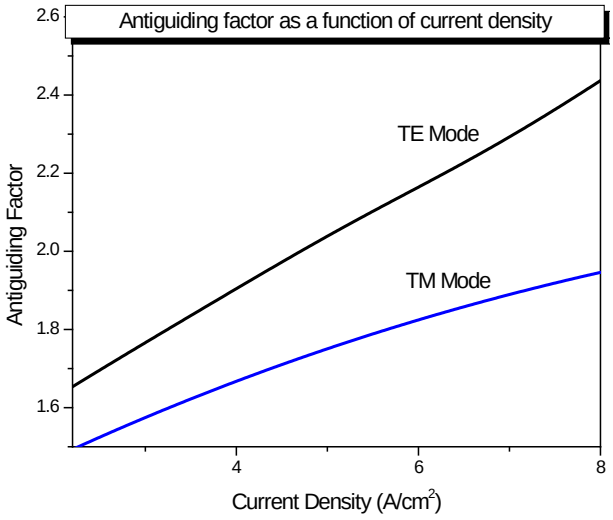

Figure 13. Anti-guiding factor as a function of current density

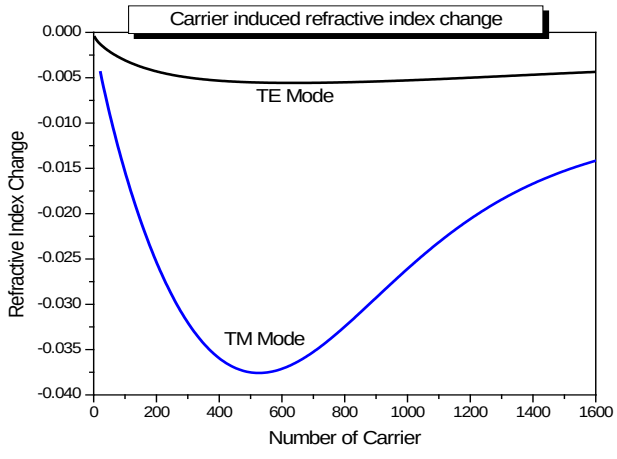

Figure 14. Refractive index profile for the TE and TM modes

Differential gain has been plotted with respect to carrier density in both modes and it is found that the variation is larger in TM mode than in TE mode as shown in Figure 15. Gain cannot be independent of the high power densities found in semiconductor lasers. Spatial hole burning and spectral hole burning are the two known phenomena which cause the gain to 'compress'. Both depend on optical power. Spatial hole burning occurs as a result of the standing wave nature of the optical modes. Increasing the lasing power means that the stimulated recombination time becomes shorter. Carriers are therefore depleted faster causing a decrease in the modal gain; while spectral hole burning is attributed to the broadening of gain profile. In Figure 16, we have plotted gain compression in TE mode against carrier density.

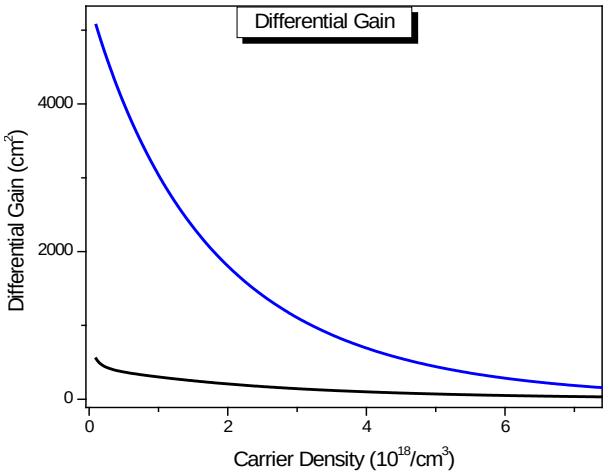

Figure 15. Plot of differential gain as a function of carrier density

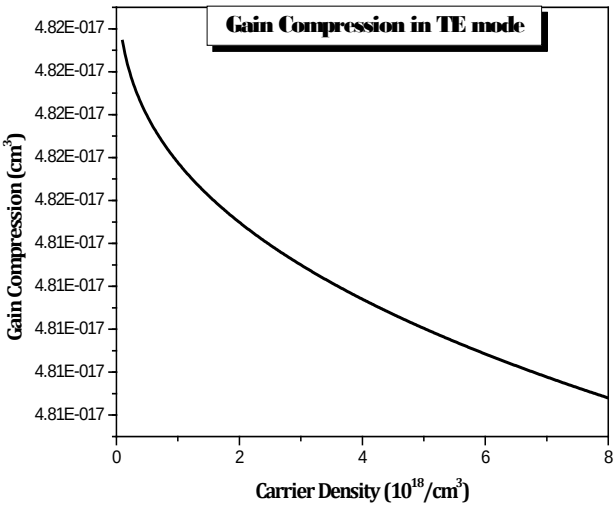

Figure 16. Gain compression plotted as a function of carrier density

5. Conclusion

We have studied various characteristics of $Al_{0.15}In_{0.22}Ga_{0.63}As/GaAs$ strained single quantum well based Graded Index (GRIN) - separate confinement lasing nano-heterostructure. For the structure, the maximum optical gain has been observed to be 5557.18 cm^{-1} at the lasing wavelength ~ 0.90 μm and photonic energy ~ 1.36 eV in TE mode and it is only 2760.70 cm^{-1} at the lasing wavelength ~ 0.78 μm and at photonic energy ~ 1.58 eV in TM mode. The maximum modal gain has been observed to be 54.65 cm^{-1} in TE mode and it is 27.16 cm^{-1}

in TM mode at the same lasing wavelengths and photonic energies respectively. The observed gain shows the usefulness of the structure in NIR region.

References

[1] Y.S. Yong, H.Y. Wong, H.K. Yow, M. Sorel, "Systematic study on the confinement structure design of 1.5 μm InGaAlAs/InP multiple quantum well lasers", Laser Phys. 20(4),811-815, (2010).

[2] J. M. Gaines, "Compound Semiconductor Epitaxy", edited by C. W. Tu, L. A. Kolodziejshi, and U. R. McGray, MRS Symposia Proceedings No. 340, Materials Research Society, Pittsburgh, p. 419,(1994).

[3] C. Weisbuch and B. Vinter, "Quantum Semiconductor Heterostructures", Academic, New York, (1993).

[4] W. T. Tsang, "Extremely low threshold AlGaAs modified multiquantum-well heterostructure lasers grown by MBE", Appl. Phys. Lett. 39, 786 (1981).

[5] W. T. Tsang, "Extremely low threshold (AlGa)As graded-index waveguide separate-confinement heterostructure lasers grown by molecular beam epitaxy", Appl. Phys. Lett. 40, 217 (1982).

[6] D. Kasemset, C.-S. Hong, N. B. Patel and P. D. Dapkus,"Graded barrier single quantum well lasers — theory and experiment", IEEE J. Quantum Electron., Vol. QE-19, pp. 1025-30 (1983).

[7] S.W. Ryu and P.D. Dapkus, "Low threshold current density GaAsSb quantum well (QW) lasers grown by metal organic chemical vapour deposition on GaAs substrates", Electron. Lett., Vol. 36, No. 16, pp. 1387- 1388, (2000).

[8] J.C. Yong, J.M. Rorison, I.H. White "1.3 μm quantum well InGaAsP, AlGaInAs and InGaAsN laser material gain: a theoretical study", IEEE J. Quantum Electroxn, Vol. 38, No. 12, pp. 1553-1564 (2002).

[9] D. P. Sapkota, M.S. Kayastha and K. Wakita, "Proposed Model of Electric Field Effects in High-Purity GaAs at Room Temperature", Opt. Quant Electron., Vol. 4, No. 5,pp. 99-103 (2014).

[10] Carsten Rohr, Paul Abbott, Ian Ballard, James P. Connolly, and Keith W. J. Barnham, Massimo Mazzer, Chris Button, Lucia Nasi, Geoff Hill and John S. Roberts, Graham Clarke, Ravin Ginige, "InP based lattice-matched InGaAsP and strain-compensated InGaAs⁄InGaAs quantum well cells for thermohotovoltaic applications", J. of Appl. Phys., 100, 114510, (2006).

[11] Pyare Lal, Shobhna Dixit, S. Dalela, F. Rahman, and P. A. Alvi, "Gain Simulation of lasing nano-heterostructure $Al_{0.10}Ga_{0.90}As$/GaAs" Physica E: Low dimensional Systems and Nanostructures, 46, pp. 224-231, (2012).

[12] P.A. Alvi, Pyare Lal, Rashmi Yadav, Shobhna Dixit, S. Dalela, "Modal Gain characteristics of InGaAlAs/InP lasing nano-heterostructures." Superlattices and Microstructures, 61, 1-12 (2013).

[13] G. P. Agrawal, "Fiber-Optic Communication Systems", 4th Edition, Wiley Interscience, Chap. 3, (2010).

[14] C.A. Wang, J. N. Walpole, L. J. Missaggia, "AlInGaAs/AlGaAs separate-confinement heterostructure strained single quantum well diode lasers grown by organometallic vapor phase epitaxy", Appl. Phy. Lett., 58, 2208, (1991).

[15] Robert N. Hall, G. E. Fenner, J. D. Kingsley, T. J. Soltys, and R. O. Carlson, "Coherent Light Emission From GaAs Junctions", Physical Review Letters 9, pp. 366-369, (1962).

[16] T. D. Moustakas and A. Bhattacharyya, "Experimental Evidence that the Plasma-Assisted MBE Growth of Nitride Alloys is a Liquid Phase Epitaxy Process," ECS Transactions: 219th ECS Meeting, vol. 35, no. 6, pp. 63-71, (2011).

[17] T. D. Moustakas and A. Bhattacharyya, "The Role of Liquid Phase Epitaxy During Growth of AlGaN by MBE," Physica Status Solidi C, vol. 9, no. 3-4, pp. 580-583, (2011).

[18] A. Bhattacharyya, T. D. Moustakas, L. Zhou, D. J. Smith, and W. Hug, "Deep Ultraviolet Emitting AlGaN Quantum Wells with High Internal Quantum Efficiency," Applied Physics Letters, vol. 94, no. 18, article no. 181907, (2009).

[19] Y. Liao, C. Thomidis, C.-K. Kao, and T. D. Moustakas, "AlGaN Based Deep Ultraviolet Light Emitting Diodes with High Internal Quantum Efficiency Grown by Molecular Beam Epitaxy," Applied Physics Letters, vol. 98, no. 8, article no. 081110, (2011).

[20] T. D. Moustakas, Y. Liao, C-k. Kao, C. Thomidis, A. Bhattacharyya, D. Bhattarai and A. Moldawer, "Deep UV-LEDs with High IQE Based on AlGaN Alloys with Strong Band Structure Potential Fluctuations," Proceedings of SPIE, vol. 8278, (2012).

[21] Pyare Lal, Rashmi Yadav, Meha Sharma, F. Rahman, S. Dalela, P. A. Alvi, "Qualitative analysis of gain spectra of InGaAlAs/InP lasing nano-heterostructure" International Journal of Modern Physics B, Vol. 28, No. 29 (2014) pp. 1450206.

[22] Sandra R. Selmic, Tso-Min Chou, Jiehping Sih, Jay B. Kirk, Art Mantie, Jerome K. Butler, Gary A. Evans, IEEE J. On Selected Topics in Quantum Electronics, **7**, No. 2 (2001).

[23] Rashmi Yadav, Pyare Lal, F. Rahman, S. Dalela, P. A. Alvi, "Investigation of material gain of $In_{0.90}Ga_{0.10}As_{0.59}P_{0.41}$/InP lasing nano-heterostructure" International Journal of Modern Physics B, Vol. 28, No. 10 (2014) pp. 1450068.

[24] G. D. Mahan, L. E. Oliveira, "Quasi-Fermi-levels in quantum-well photoluminescence," Phys. Rev. B 44, 3150 (1991).